Comparison of Stress Distributions between Numerical Cross-Section Analysis and 3D Analysis of Tapered Beams

Bertolini, Paola; Sarhadi, Ali; Stolpe, Mathias; Eder, Martin Alexander

Published in:
Proceedings of the 2019 International Conference on Composite Materials

Publication date:
2019

Document Version
Publisher's PDF, also known as Version of record

COMPARISON OF STRESS DISTRIBUTIONS BETWEEN NUMERICAL CROSS-SECTION ANALYSIS AND 3D ANALYSIS OF TAPERED BEAMS

Paola Bertolini[1,2], Ali Sarhadi[2], Mathias Stolpe[2] and Martin A. Eder[2]

[1] LM Wind Power, Jupitervej 6, 6000 Kolding, Denmark, paola.bertolini@lmwindpower.com
[2] Technical University of Denmark, Frederiksborgvej 399, 4000 Roskilde, Denmark, asar@dtu.dk, matst@dtu.dk, maed@dtu.dk

Keywords: Tapered beam, Cross-section analysis, Stress distribution, Finite element model

ABSTRACT

While the demand for new and longer wind turbine blades is increasing, time for their design and production is shortening. 3D finite element models generally have the capability of providing a complete and detailed analysis of the behaviour of such structures. Nonetheless, computationally efficient and accurate cross-section analysis tools are required to improve the efficiency of the workflow in the conceptual design phase. Several cross-section analysis software, such as BEam Cross-Section Analysis Software BECAS, have been developed for analysis of prismatic beams. As a result, structures which are tapered along their longitudinal axis, i.e. aircraft wings or wind turbine blades, are modelled as step-wise prismatic beams and the known effects on stresses due to taper are ignored. This study provides a numerical comparison of the Cauchy's stress components evaluated with both 3D finite element and cross-section analysis consisting of linear elastic isotropic and anisotropic materials. Results highlight how every cross-section formulation that relies on the step-wise prismatic assumption lacks the capability to correctly recover the stresses in tapered beams.

1 INTRODUCTION

Nowadays, aerospace and wind energy industries are facing new challenges related to an upscaling tendency of aircrafts and wind turbine rotors, where low costs of production and optimal structural designs must be assured. In such cases, advanced composite materials and lengthwise geometrical variations (LGVs) play a key role. Aircraft structures and wind turbine blades are typically made from glass/carbon-fibre polymer composite beams and comprise of lengthwise geometrical variations LGVs such as pre-curved beam axis and twist and variation of the dimensions of their cross section from the root to the tip, i.e. taper [1]. Material anisotropy and LGVs induce material and geometry coupling, respectively. This study is concerned only with geometrical coupling due to taper.

Among the LGVs, taper is defined as the variation of the dimensions of the cross section along the longitudinal axis of the beam [2]. The effects of taper in beams have been noticed since the last century, when studies on a planar isotropic wedge loaded at its tip showed a non-trivial shear stress distribution [3, 4]. Recently, Bennati et al. [5] focused on the analysis of a planar truncated isotropic beam under axial and shear load as well as bending moment, highlighting how the maximum shear stress does not necessarily occur at the cross-section centre-line in tapered beams. Bertolini et al. [2] derived a methodology to describe the full Cauchy's stress field in thin-walled tapered beams. Balduzzi et al. [6] studied the variation of the stress distribution in planar anisotropic tapered beams. The aforementioned studies revealed that taper effects are not negligible in beam design and that they are not captured in classic beam models.

In wind turbine manufactory industries, the blade designs are constantly and rapidly changing to answer to the costumers' demand. For this reason, accurate and computationally efficient analysis tools to perform aero-elastic and structural analysis are required. Even though 3D finite element analyses are able to model LGVs, they are too computationally expensive to be employed in the above-mentioned analyses. Since wind turbine blades have a high length-to-height and length-to-width ratio, they can be modelled as slender beams.

Nowadays the above-mentioned cross-section analysis can be accomplished by different design tools, such as VABS [7], which is based on the variational asymptotic method, ANBA [8] and BECAS [9], which are both based on the anisotropic beam theory developed by Giavotto et al. [10]. They provide the six-by-six stiffness matrix of the cross-section of a slender linear elastic anisotropic prismatic beam for small strains and displacements used for aeroelastic analysis. On the other hand, they can be used to recover stresses and strains in cross sections when the internal forces are known e.g. from aeroelastic analysis. The aforementioned cross-section analysis tools use the definition of the energy per unit beam length under the assumption of prismatic beam geometries. Therefore, tapered beams are approximated as step-wise prismatic beams and the recovered stress field lacks the effects of taper previously mentioned.

The objective of the present work is to investigate how cross-section analysis could over/under-estimate the stress field in a tapered beam. Tapered homogeneous isotropic and anisotropic beams with four different cross-sections and subjected to an external shear force are modelled with 3D finite element and cross-section analyses to compute the Cauchy's stress components. The numerical comparison between the two solutions highlight how the latter fails to capture some of the stress components as well as to predict the stress distribution correctly.

2 METHOD

A 3D finite element model of a tapered cantilever beam loaded by an external shear force is created to extract the stresses at its middle section. The results are numerically compared with the ones evaluated by cross section analysis in the cross section at the mid-span. The latter is subjected to the internal forces induced by externally applied load. The software BECAS developed at DTU Wind Energy is used for cross-section analysis and the commercial finite element package Abaqus [11] for the numerical analysis of the 3D finite element model.

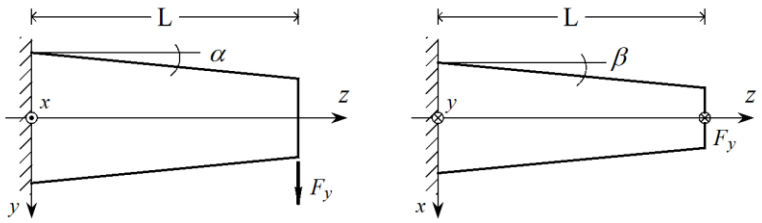

Figure 1: Side and top view of the analyzed doubly tapered beams. The beam presents a constant vertical taper α and horizontal taper β. The DOFs in the plane at z = 0 are constrained and the load is applied at z = L.

Four tapered cantilever beams are considered. They are represented in the coordinate system *Oxyz* as illustrated in Fig. 1. The beams have length L and constant vertical and horizontal taper angles, named α and β respectively. As demonstrated in Bertolini et al. [2], a thin-walled tapered homogeneous isotropic beam exhibits taper effects under axial or shear force or bending moment. Aircraft wings and wind turbine blades experience a combination of aerodynamic-gravitational-inertial loads during operation life [1]. Bending in the direction perpendicular to the blade axis (flapwise) is one of the main load cases. Therefore, for simplicity, this paper analyses cross sections which are subjected only to an internal shear force and bending moment. Small taper angles (see Table 2) have been used to allow the comparison of the isotropic thin-walled rectangular model with the analytical solution provided in [12].

The analysed tapered beams involve four different cross sections, as described in the following. Two homogeneous isotropic tapered beams with solid rectangular cross section (ISR) and thin-walled rectangular cross section (ITWR); two anisotropic tapered beams with thin-walled rectangular cross section (CTWR) and with blade-like cross section (CB). The latter is a combination of a semicircle and a trapezoid.

In order to solely investigate the geometrical coupling caused by taper, the fibre directions in the rectangular cross section are chosen in such a way to eliminate any source of anisotropy material

coupling. Moreover, analytical solutions for ITWR tapered beams are available in the literature [2, 12] and they will be used for comparison in this study. The blade-like cross section is chosen to analyse a more realistic example. Aluminum, which is widely used in aircraft industries, and E-glass/epoxy lamina, which is typically used in wind turbine blades, are employed to investigate the relation between taper and linear isotropic and linear anisotropic materials, respectively. The properties of the two materials are listed in Table 1. For simplicity, the flanges of CTWR as well as the flanges and the leading edge of CB are uniaxial E-glass/epoxy laminate and the webs of both models are [+45° -45° +45°] laminate.

Material	E_{11} [GPa]	$E_{22}=E_{33}$ [GPa]	$G_{12}=G_{13}$ [GPa]	G_{23} [GPa]	$\nu_{12}=\nu_{13}$	ν_{23}	ρ [Kg/m^3]
Aluminium	70	70	26	26	0.3	0.3	2700
E-glass/ epoxy	39.5	12.10	4.54	4.54	0.275	0.333	1845

Table 1: Properties of the isotropic (aluminium) and of the composite materials (E-glass/ epoxy [1]).

In order for the model from BECAS to be comparable to the one from Abaqus, a reference cross section located at the midspan of each cantilever beam is considered. Being the reference cross section sufficiently far from the clamped root and the loaded tip, the influence of the boundary effects becomes negligible. Moreover, the reference cross sections are chosen perpendicular to the beam axis and located at z = 5 m. Their geometrical dimensions are given in Table 2.

Model	L [m]	B [mm]	H [mm]	t [mm]	α [deg]	β [deg]
ITWR	10	1000	1200	24	2.5	1.5
CTWR	10	1000	1200	24	2.5	1.5
ISR	10	1000	1175	-	2.5	1.5
CB	10	300	600	24	1.2	3.4

Table 2: Geometrical dimensions of the four beams.

The mesh discretization of the four models is shown in Fig. 2 and 3. The number of elements in each part of the cross section and the total number of elements of the Abaqus and BECAS models are given in Table 3.

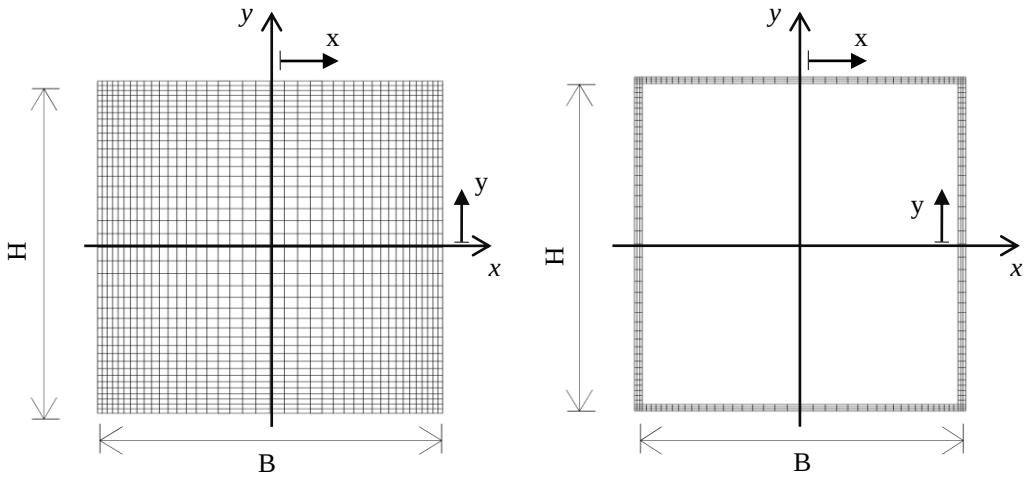

(a) (b)

Figure 2: Finite element mesh of the cross sections (a) ISR and (b) ITWR. The local directions x and y indicates the directions of the paths along which the stresses are extracted.

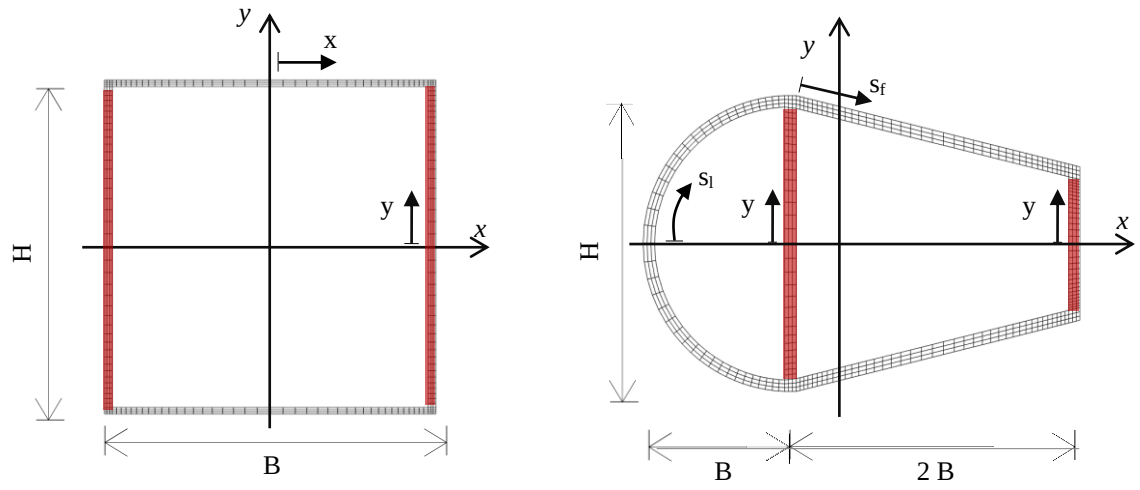

(a) (b)

Figure 3: Finite element mesh of the cross sections (a) CTWR and (b) CB. The coloured webs have direction [+45° -45° +45°]. The local directions x, y, s_f, and s_l indicates the directions of the paths along which the stresses are extracted.

	ISR		ITWR		CTWR		CB	
	# el	bias-ratio	# el	bias-ratio	# el	bias-ratio	# el	bias-ratio
Flange	40	3	40	2	40	2	50	2
Flatback	40	3	40	2	40	2	20	1
Internal web	-	-	-	-	-	-	50	2
Leading edge	-	-	-	-	-	-	80	2
Length	180	4	180	4	180	4	120	2
Total #el in Abaqus	80 000		51 600		51 600		46 080	
Total #el in BECAS	1 600		516		516		576	

Table 3: Number of elements and ratio of the size of the coarsest element to the size of the finest element (bias-ratio) in each part of the cross sections. 'Length' refers to the number of elements along the span of the beam. The total number of elements in the two models is also given.

2.1 3D finite element model

The 3D finite element models were discretised with incompatible mode eight-noded brick elements (Abaqus element type C3D8I). Convergence studies were performed by refining the mesh until a mesh-independent solution was achieved. They are omitted in this paper for the sake of brevity. As shown in Fig. 2 and 3, the mesh of the cross sections was refined close to the corners to increase the accuracy of the evaluated stress field in the proximity of the singularities. For the two examples CTWR and CB, each laminate was modelled from partitioning the wall thickness in the three laminae and by assigning the material orientation as designed. The materials properties are defined in Table 1.

The external load and the clamped condition were applied through a reference point located at the geometrical centroid of the tip and the root. These reference points were then constrained to the surfaces at the tip and the root using kinematic couplings. The Abaqus linear perturbation solver was used. After defining a nodal path, the stresses were extracted in global coordinates in ISR and ITWR, and in the material coordinates in CTWR and CB, as defined in the Results Section.

2.2 Cross section model

The software BECAS provides the six-by-six cross-section stiffness matrix, the shear and elastic centres of any anisotropic cross-section and arbitrary geometry. Given as input the geometry of a cross section, the properties of the materials and the internal forces, a finite element model of the cross section was created and analysed. The cross sections of this study were modelled with four-noded 2D plane elements (Q4), coherently with the chosen linear elements used in the Abaqus model. The applied internal forces were equivalent to the ones caused by the tip load applied in the models in Abaqus and they are given in Table 4.

External force	Internal forces	
Shear force	Shear force	Bending moment
1000 N	1000 N	-5000 Nm

Table 4: Internal forces at the reference cross sections due to the external load F_y applied at the tip.

3 RESULTS AND DISCUSSION

The Cauchy's stresses were evaluated at the centroid of each element in the 3D FEM from Abaqus and in the model from BECAS. To validate the models from BECAS, each cross section was modelled as prismatic 3D finite element in Abaqus. The stress components in the three different models provide a numerical comparison of the effects of LGVs.

The cross sections of ISR, ITWR, CTWR have two axes of symmetry, therefore the stress distributions are symmetric, and it suffices to show to show them along a quarter of the cross section ($0 < x < B/2$ and $0 < y < H/2$). Results from CB are reported only for half of the cross-section ($0 < y < H/2$). In Fig. 4 - 13 the label 'BECAS CS' refers to the results from BECAS, '3D CSP' and '3D CST' to the ones from the prismatic and tapered models in Abaqus respectively.

3.1 ISR: a solid rectangular cross-section with homogeneous isotropic material

A doubly tapered cantilever beam with solid rectangular cross section was modelled and analysed. The comparison in Fig. 4 and 5 refers to a vertical and to a horizontal path located at $x = 0.49$ m and $y = 0.57$ m respectively. Stresses are evaluated in the global coordinate system *Oxyz*.

In a cross section of a homogeneous isotropic prismatic beam with solid rectangular cross section subjected to internal shear and shear-bending, only axial and in-plane shear stresses arise. Figures 4 and 5 show that if the same beam is slightly tapered none of the stress components is zero.

As expected [13], the axial stress component σ_{zz} in both the vertical and horizontal path is not affected by taper. The other stresses σ_{xx}, σ_{xy}, σ_{xz}, σ_{yy} are strongly at variance and they increase when moving toward the edge of the cross section. For example, the shear stress distribution along the vertical path of the prismatic beam reaches its maximum value at the mid-span, whereas it occurs at the extremity of the cross section in the tapered beam, as experienced in homogeneous isotropic thin-walled cross sections [2].

3.2 ITWR: a thin-walled rectangular cross-section with homogeneous isotropic material

The stresses along the web and flange of the current cross section are evaluated in the global coordinate system *Oxyz*. Three different methods were applied: the cross-section analysis BECAS, the 3D finite element model in Abaqus, and the closed-form analytical solutions ('Analytical') provided in Bertolini and Taglialegne [12]. Analytical solutions and Abaqus models of the tapered beams are in good agreement and they are both able to capture the effects of taper. As in the previous example, the axial stress component σ_{zz} in the flange and the web is hardly affected by small taper angles [13]. On the other hand, the shear stress distributions are wrongly predicted in BECAS because the shear-bending coupling caused by the taper is not depicted. It reduces the shear stress σ_{yz}, but it also shifts its

maximum from the mid-span to the corner, as shown in Fig. 7-e. In addition, the stress components σ_{xx}, σ_{xz}, σ_{yy} are not zero even for the small taper angles used in this model.

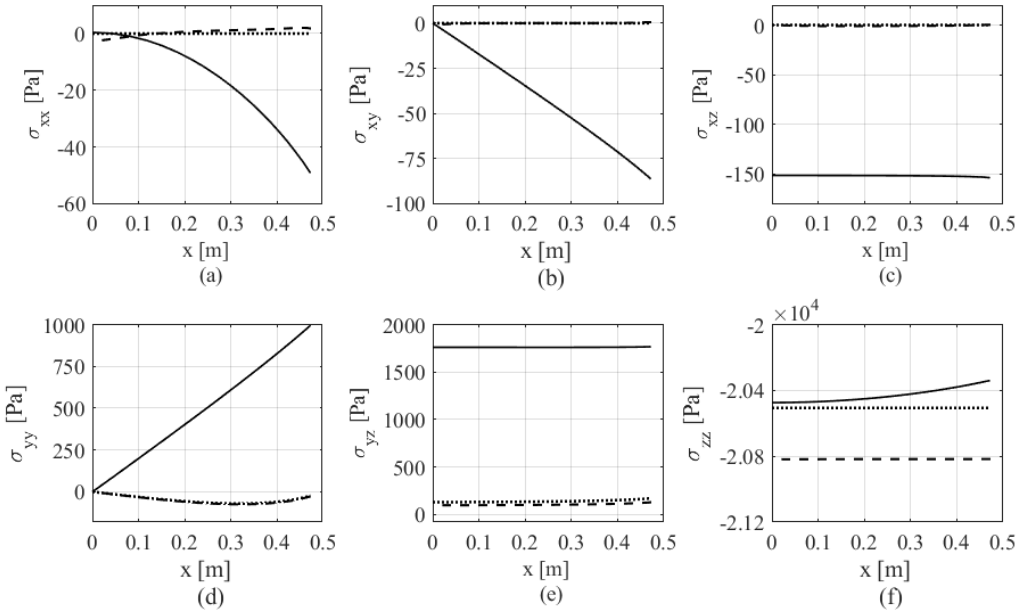

Figure 4: Stress distributions along a horizontal path located in the proximity of the edge of model ISR under an external shear force. Legend: --- BECAS CS, — 3D CST, ····· 3D CSP.

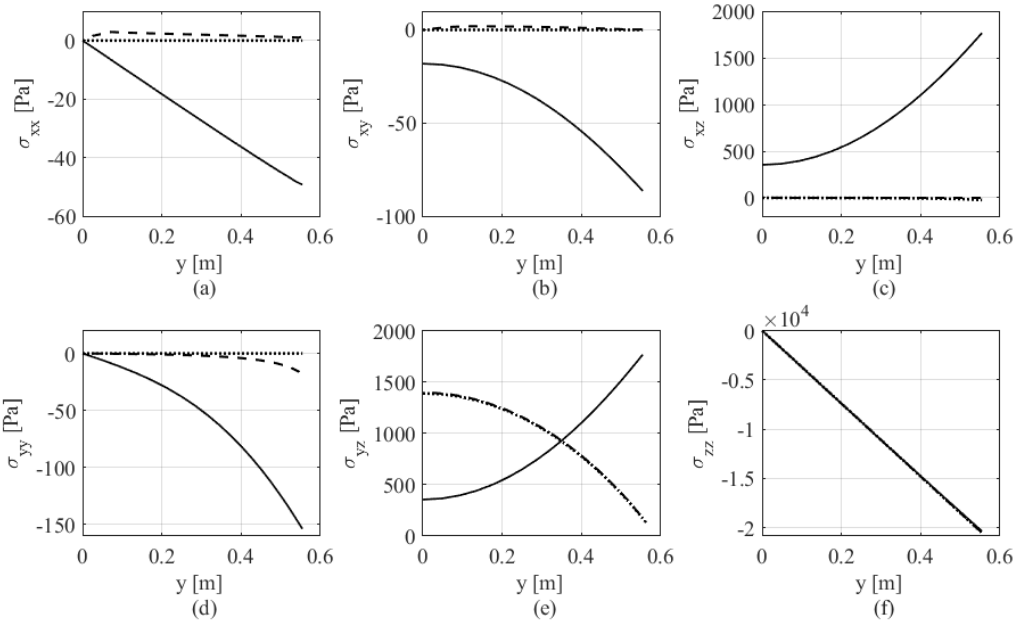

Figure 5: Stress distributions along a vertical path located in the proximity of the edge of model ISR under shear force. Legend: --- BECAS CS, — 3D CST, ····· 3D CSP.

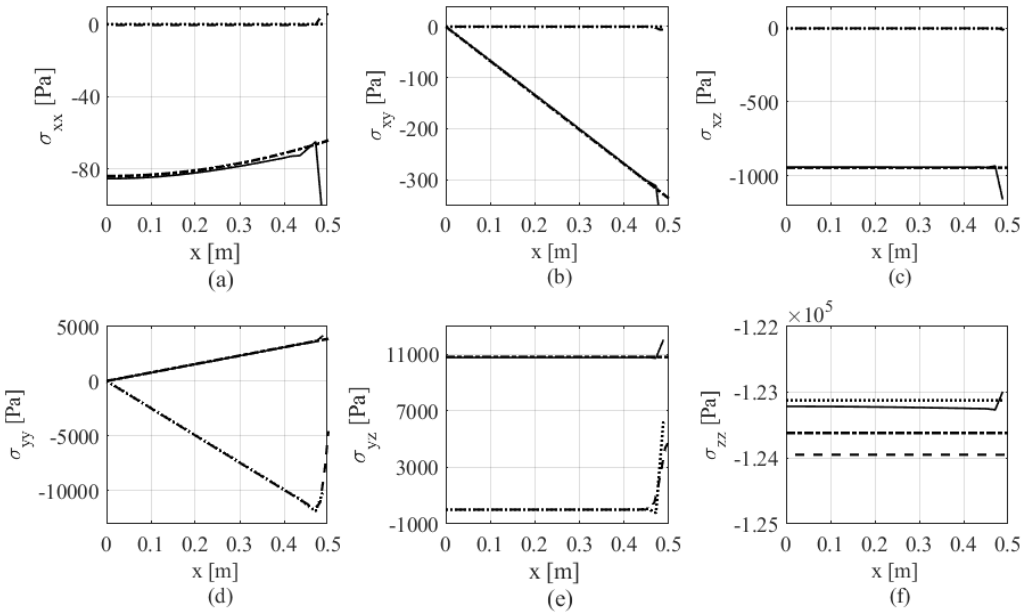

Figure 6: Stress distributions along the flange of model ITWR under shear force.
Legend: --- BECAS CS, — 3D CST, ····· 3D CSP, ·-·-· Analytical.

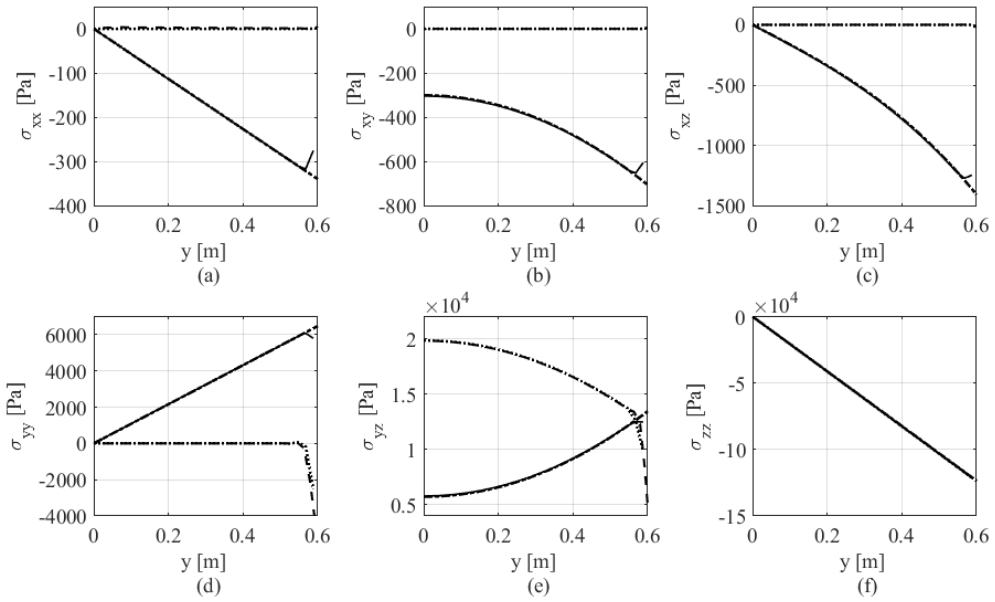

Figure 7: Stress distributions along the web of model ITWR under shear force.
Legend: --- BECAS CS, — 3D CST, ····· 3D CSP, ·-·-· Analytical.

3.3 CTWR: a thin-walled rectangular cross-section with composite material

The same cross section analysed in the previous section is now composed by three laminae of E-glass/epoxy. In the flanges, the fibres are oriented along the beam direction $(0°)_3$ and in the webs, the plies have direction angles [+45° -45° +45°]. The stresses are therefore evaluated in the material coordinate system *O123*, where the axis corresponding to the 1-direction is aligned with the fibres and the axis corresponding to the 3-direction is the outward normal. Figure 8 shows the stresses in half of

the internal lamina of the flange. It is worth noting that the axial stress σ_{11} and the-out-of-plane components are not affected by taper. The in-plane shear stress has opposite sign and it is three times overestimated in BECAS.

Figure 9 shows the stresses in the internal lamina of the web where the fibres have direction -45°. In this case, BECAS correctly predicts the in-plane shear stress σ_{12}, whereas it overestimates the in-plane stress components σ_{11} and σ_{22} by three-times in comparison to Abaqus. In addition, taper induces the out-of-plane stress components, which are zero in the prismatic case. Out-of-plane stresses have a key role in failure design because they are involved in delamination of the laminate. It is worth noting that even if σ_{13} and σ_{23} are 10 times smaller than σ_{12}, the transverse tensile strength is typically 20 times smaller than the longitudinal tensile strength in unidirectional laminae [14]. Therefore, the ratios stresses-to-strength in the transverse and longitudinal direction are comparable.

3.4 CB: a wind turbine blade cross sectional geometry of composite material

The last example is a tapered cantilever beam with the blade-like cross section given in Fig. 3-b. The airfoil is made of three-layer uniaxial laminate and the webs of three-layers laminate with ply angles of $[+45° \ -45° \ +45°]_3$. Stresses are computed in the material coordinate system *O123*, which is defined in such a way that the fibres follow the 1-direction and the 3-direction is outward normal to the laminate. The numerical comparison refers only to the stresses along the upper flange in Fig. 10, the leading edge in Fig. 11, and half of the webs in Fig. 12 and 13 are presented.

Results from BECAS and the prismatic FEM in Fig. 10 show that only axial and in-plane shear stresses occur in the upper flange. When the beam is tapered, the axial stress σ_{11} slightly increases and the shear stress σ_{12} is strongly reduced and has a different distribution with maximum value $s_f = 0$ and quasi-zero stress at the external corner ($s_f \rightarrow 0.8$m). Among the remaining components, the out-of-plane stresses are not zero in the tapered model and the maximum value of σ_{23} has the same order of magnitude as σ_{12}. The combination of such a high transverse shear stress in Fig. 10-e and transverse tensile stress in Fig. 10-f , might be critical in delamination of the laminate or debonding of the adhesive joint, as already pointed out in the previous section.

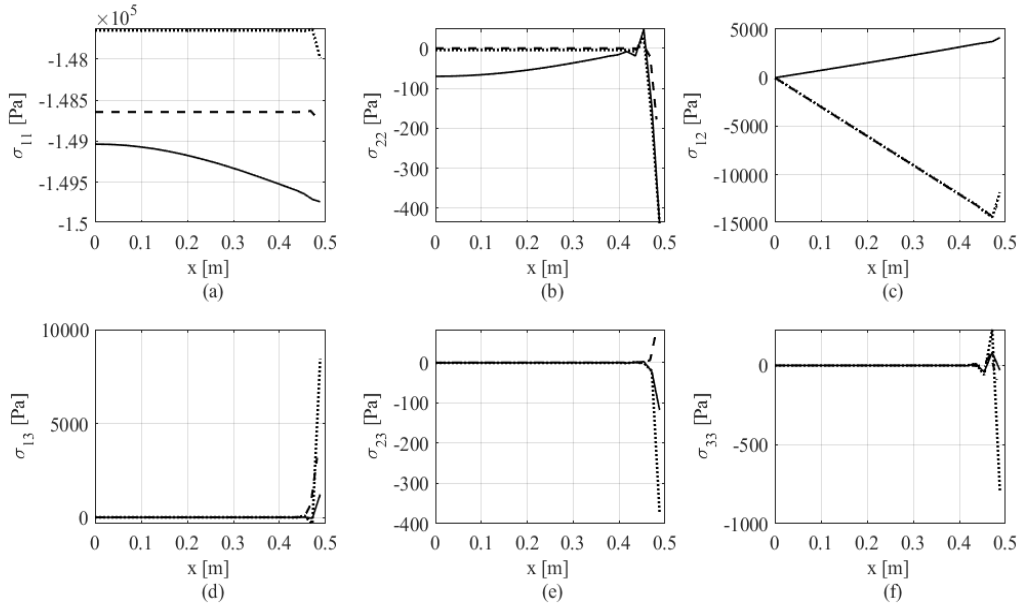

Figure 8: Stress distributions along half of the flange of model CTWR loaded by a shear force. The stresses are from the internal lamina (0°).
Legend: --- BECAS CS, — 3D CST, ····· 3D CSP.

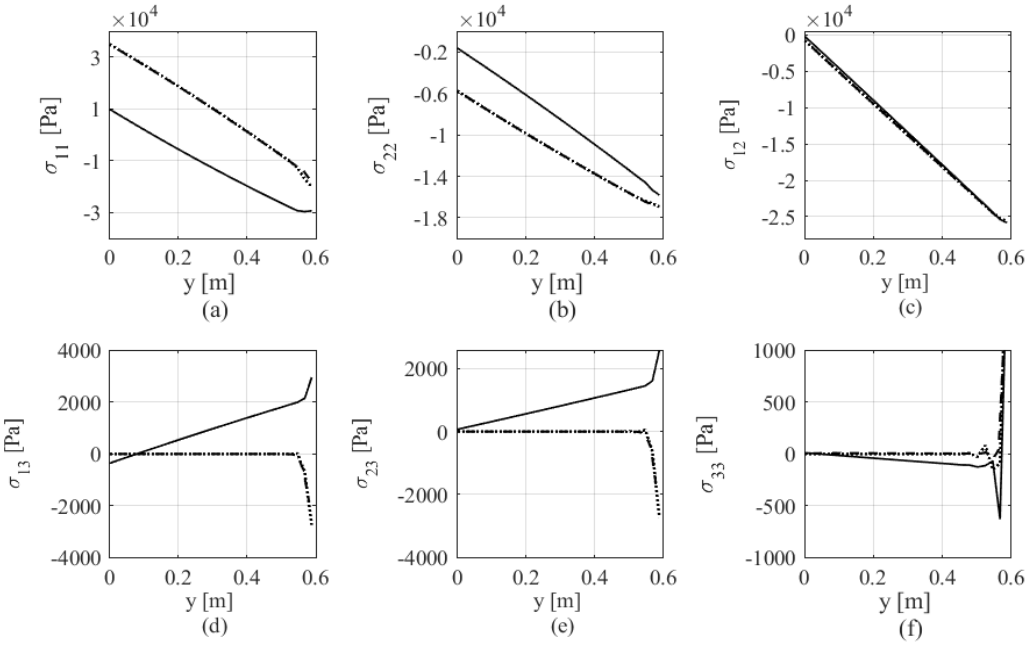

Figure 9: Stress distribution along half of model CTWR loaded by a shear force. The stresses from the internal lamina (-45°). Legend: --- BECAS CS, — 3D CST, ····· 3D CSP.

Figure 11 refers to half of the leading edge. Only axial and in-plane shear stresses arise in the prismatic case. In the tapered model the axial stress does not change, whereas the in-plane shear stress halves and $\sigma_{12} = 0$ at $s_l = 0.3$ m. As observed in the flange of CB, the out-of-plane shear stress σ_{23} in Fig. 11-e has values comparable to the in-plane shear stress at the intersection between the leading edge, the flange and the internal web. Delamination could have a driving role in the failure design. The distribution of σ_{13} shown in Fig. 13-d does not provide sufficiently accurate results. Indeed, results from BECAS deviate from the prismatic model in Abaqus and therefore a deeper investigation is needed.

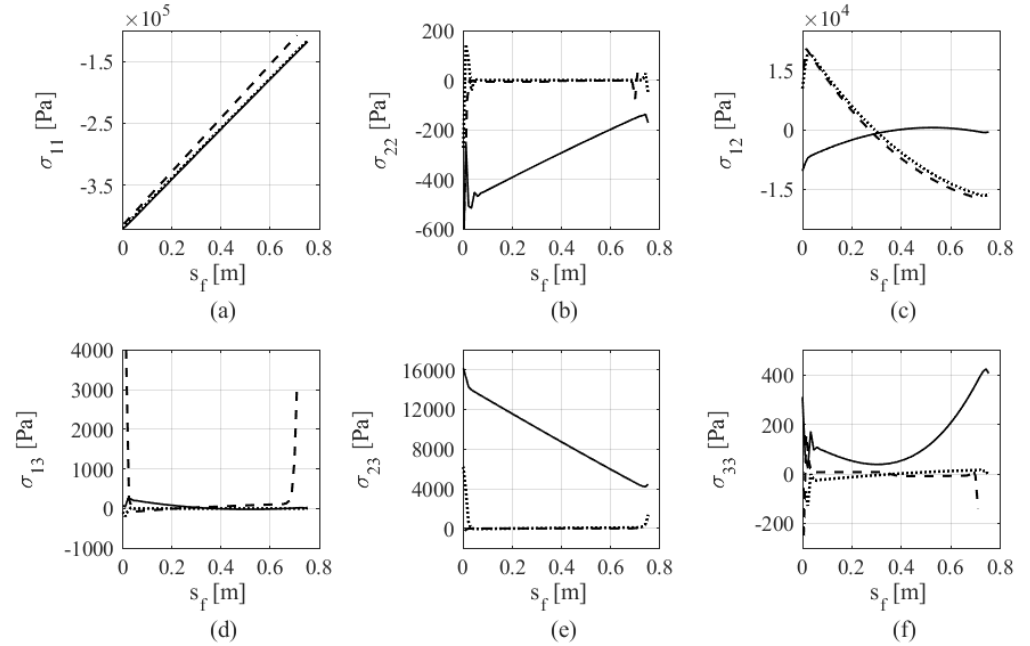

Figure 10: Stress distribution along the upper flange of model CB under a shear force. The stresses are extracted in the internal lamina (0°). Legend: --- BECAS CS, — 3D CST, ····· 3D CSP.

Figure 12 shows the stresses in the web along the external lamina (+45°). The in-plane shear stress σ_{12} from the three models is the same, the axial component σ_{11} is overestimated in BECAS, whereas the σ_{22} is underestimated. As in the previous cases, the out-of-plane stresses are not zero when the beam is tapered. In the beam analysed in this study, the transverse shear components in Fig. 12-d and Fig. 12-e are circa four or six times smaller than the in-plane shear component, but as explained before, delamination could be crucial.

Similar observations can be drawn for the flatback, whose stress components are shown in Fig. 13. The component σ_{12} is not affected by the taper, whereas σ_{11} and σ_{22} are overestimated in BECAS. Delamination failure may be critical also in this region, since the out-of-plane shear stresses in Fig. 13-d and Fig. 13-e are not zero.

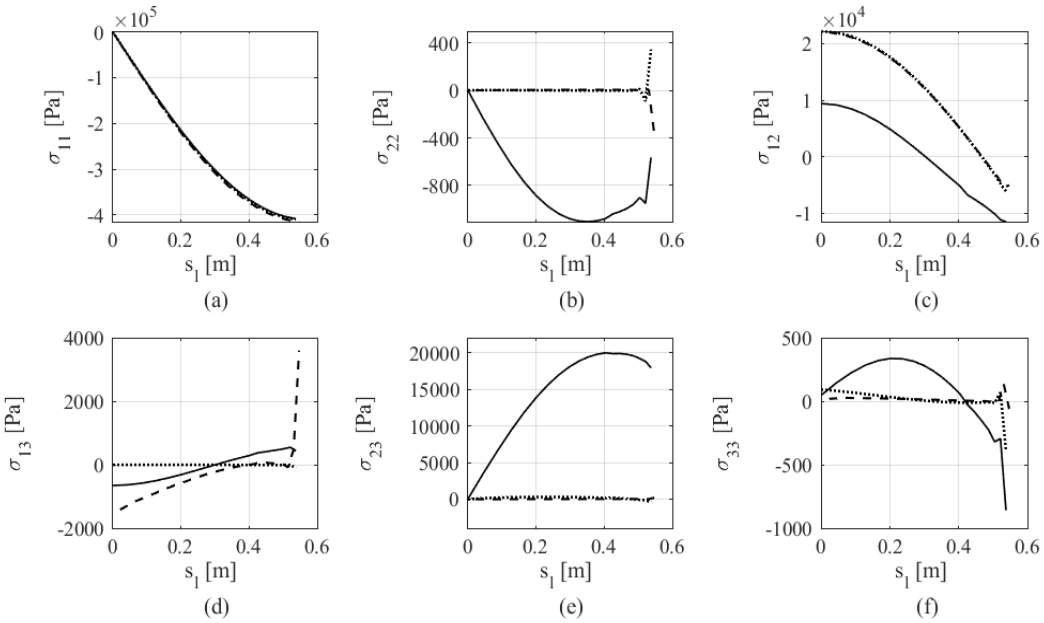

Figure 11: Stress distribution along the leading edge of model CB under a shear force. The stresses are extracted in the internal lamina (0°). Legend: --- BECAS CS, — 3D CST, ····· 3D CSP.

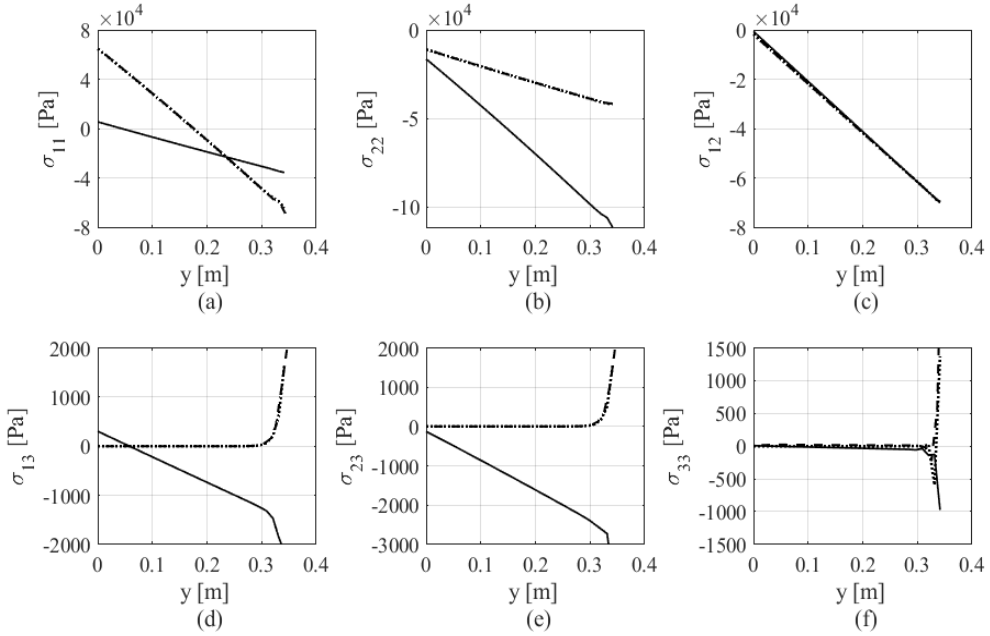

Figure 12: Stress distribution along the internal web of model CB under a shear force. The stresses are extracted in the external lamina (+45°). Legend: --- BECAS CS, — 3D CST, ····· 3D CSP.

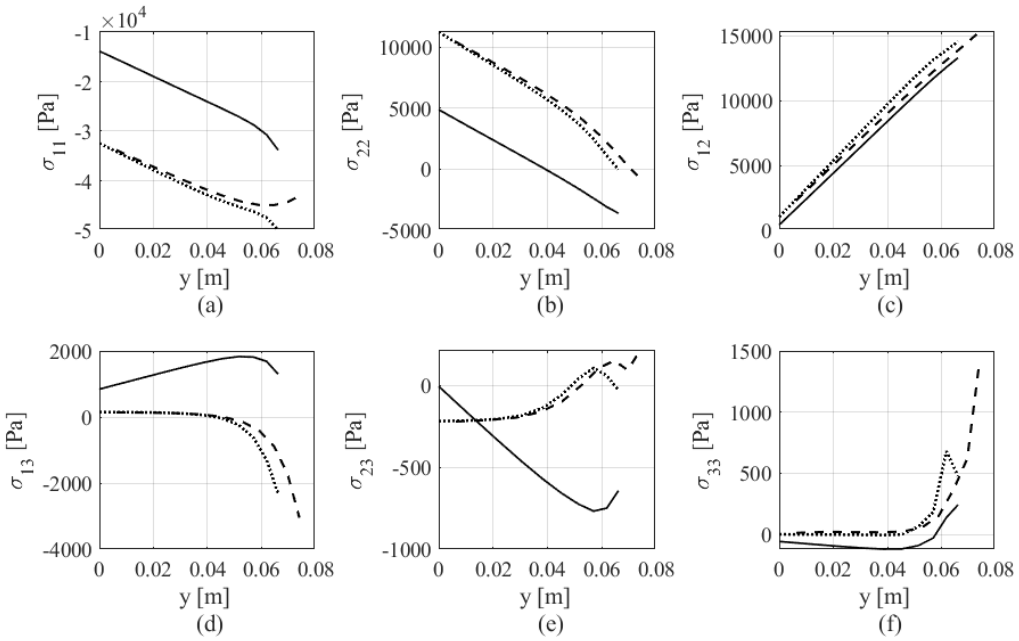

Figure 13: Stress distribution along the flatback of model CB under a shear force. The stresses are extracted in the internal lamina (-45°). Legend: --- BECAS CS, — 3D CST, ····· 3D CSP.

9 CONCLUSIONS

In this paper the Cauchy stress distributions in tapered cantilever beams subject to concentrated shear loads are compared with stress distributions recovered from cross-section analysis induced by equivalent internal cross section forces. In this study three different cross section geometries are investigated where both isotropic and anisotropic material behaviour is considered. The aim of this study is to shed light on the deviation between the stress fields in tapered 3D finite element models and those provided by stepwise prismatic cross-section analysis models. The following conclusions can be drawn from the results:

1. The numerically predicted stress distributions obtained by both, 3D analysis and cross-section analysis agreed well in all prismatic cases. The analytically obtained stress distributions agreed well with those predicted by 3D analysis in the designated tapered cases.
2. The stepwise prismatic approach adopted in the cross-section analysis methods incorrectly predicts the stresses provided by tapered 3D finite element models. The stress distributions in tapered cross sections were found to be significantly at variance where the magnitude of deviation is a strong function of the taper angle.
3. The deviations occur for any taper angle different from zero irrespective of isotropic or anisotropic material behaviour. The taper can significantly augment the stress distributions prevailing in prismatic cases whence the deviations are typically counterintuitive.
4. Particularly relevant for fibre-polymer composites it was demonstrated that taper is prone to induce through thickness transverse tensile stress components. Such peeling stress components have the propensity to significantly affect the fatigue life of composites.

ACKNOWLEDGEMENTS

This work was conducted within the industrial PhD project 'Advanced Accurate and Computationally Efficient Numerical Methods for Wind Turbine Rotor Blade Design' [grant number: 5189-00210B] funded by Innovation Fund Denmark and LM Wind Power. The financial support is gratefully acknowledged.

REFERENCES

[1] C. Bak, F. Zahle, R. Bitsche, A. Yde, L.C. Henriksen, A. Nata and M.H. Hansen, The DTU 10-MW reference wind turbine, *Danish Wind Power Research 2013,* 2013.

[2] P. Bertolini, M.A. Eder, L. Taglialegne and P.S. Valvo, Stresses in constant tapered beams with thin-walled rectangular and circular cross sections, *Thin-Walled Structures*, **119**, 2019, pp. 527-540.

[3] S.P. Timoshenko, J.M. Gere, *Mechanics of materials*, Van Nostrand Reinhold, New York, 1972.

[4] J.H. Michell, Elementary distributions of plane stress, *Proceedings of the London Mathematical Society*, **s1-32**, 1900, pp. 247-257.

[5] S. Bennati, P. Bertolini, L. Taglialegne and P.S. Valvo, On stresses in tapered beams (submitted).

[6] G. Balduzzi, M. Aminbaghai F. Auricchio and J. Füssl, Planar Timoshenko-like model for multilayer non-prismatic beams, *International Journal of Mechanics and Materials in Design*, **14**, 2017, pp.51-70.

[7] C.E. Cesnik and D.H. Hodges, VABS: a new concept for composite rotor blade cross-sectional modeling, *Journal of the American Helicopter Society*, **42**, 1997, pp. 27-38.

[8] M. Morandini, M. Chierichetti and P. Mantegazza, Characteristic Behavior of Prismatic Anisotropic Beam Via Generalized Eigenvectors, *International Journal of Solids and Structures*, **47**, 2010, pp. 1327-1337.

[9] P. Blasques, R. Bitsche, V. Fedorov and M.A. Eder, Applications of the BEam Cross-section analysis Software (BECAS), *Proceedings of the 26th Nordic Seminar on Computational Mechanics*, 2013, pp. 46-49.

[10] V. Giavotto, M. Borri, P. Mantegazza and G. Ghiringhelli, Anisotropic beam theory and applications, *Computer & Structures*, **16**, 1983**,** pp. 403-413.

[11] ABAQUS 2017, Dassault Systemes Simulia Corporation, 2018.

[12] P. Bertolini and L. Taglialegne, Analytical expressions in doubly tapered beams (submitted).

[13] B.A. Boley, On the accuracy of the Bernoulli-Euler theory for beams of variable section, *Journal of Applied Mechanics*, **30**, 1963, pp. 373–378.

[14] E.J. Barbero, *Composite Materials Design*, CRC press, Boca Raton, 2017.